

Electronic supplementary information

**A hybrid nanosensor based on novel fluorescent iron oxide nanoparticles
for highly selective determination of Hg²⁺ ion in environmental samples**

Süreyya Oğuz Tümay*, Vildan Şanko, Ahmet Şenocak, Erhan Demirbas

Department of Chemistry, Gebze Technical University, Gebze 41400, Kocaeli, Turkey

* Corresponding authors:

Dr. Süreyya Oğuz TÜMAY, Department of Chemistry, Gebze Technical University, P.O. Box:
141, Gebze 41400, Kocaeli, Turkey

Tel: 00 90 262 6053106

Fax: 00 90 262 6053105

e-mail: sotumay@gtu.edu.tr

The caption of content:

Figure S1: a) ^1H NMR, b) ^{13}C NMR and c) FTIR spectra of compound **1**. (NMR spectra were recorded in CDCl_3).

Figure S2: a) MALDI-TOF b) ^1H NMR, c) ^{13}C NMR and d) FTIR spectra of compound **2**. (MALDI-MS spectrum was obtained with dithranol matrix and NMR spectra were recorded in DMSO-d_6).

Figure S3: FTIR spectra of compound **2**, $\text{AP@SiO}_2\text{@Fe}_2\text{O}_3$, $\text{Py@Fe}_2\text{O}_3$ hybrid nanosensor.

Figure S4: UV-Vis spectra of compound **2**, $\text{SiO}_2\text{@Fe}_2\text{O}_3$, $\text{AP@SiO}_2\text{@Fe}_2\text{O}_3$, $\text{Py@Fe}_2\text{O}_3$ hybrid nanosensor.

Figure S5: TGA thermograms of compound **2**, Fe_2O_3 , $\text{SiO}_2\text{@Fe}_2\text{O}_3$, $\text{AP@SiO}_2\text{@Fe}_2\text{O}_3$, $\text{Py@Fe}_2\text{O}_3$ hybrid nanosensor.

Figure S6. XRD patterns of Fe_2O_3 , $\text{AP@SiO}_2\text{@Fe}_2\text{O}_3$, $\text{Py@Fe}_2\text{O}_3$.

Figure S7. UV-Vis absorption of $\text{Py@Fe}_2\text{O}_3$ in a) hexane, b) 1,4-dioxane, c) THF, d) dichloromethane, e) ACN, f) ethanol, g) DMSO, h) DMF, i) water in different concentration and j) normalized absorption spectra of $\text{Py@Fe}_2\text{O}_3$ in different solvents.

Figure S8. Fluorescence spectra of $\text{Py@Fe}_2\text{O}_3$ in a) hexane, b) 1,4-dioxane, c) THF, d) dichloromethane, e) ACN, f) ethanol, g) DMSO, h) DMF, i) water in different concentration and j) normalized fluorescence spectra of $\text{Py@Fe}_2\text{O}_3$ in different solvents.

Figure S9. Interfering studies for 0.4 mg.mL^{-1} $\text{Py@Fe}_2\text{O}_3$ in presence of $1.0\text{ }\mu\text{mol.L}^{-1}$ Hg^{2+} after addition of $10\text{ }\mu\text{mol.L}^{-1}$ various competitive species (pH of 8.0, $\lambda_{\text{ex}}=325\text{ nm}$, and slit width = 5 nm).

Figure S10. Effect of a) pH, b) buffer concentration, c) $\text{Py@Fe}_2\text{O}_3$ concentration, d) photostability and e) measurement time at pH of 8.0, $\lambda_{\text{ex}}=325\text{ nm}$, 0.4 mg.mL^{-1} of $\text{Py@Fe}_2\text{O}_3$ and $1.0\text{ }\mu\text{mol.L}^{-1}$ Hg^{2+} , and slit width = 5 nm).

Table S1: Photophysical parameters of $\text{Py@Fe}_2\text{O}_3$.

Table S2. Optimum conditions of $\text{Py@Fe}_2\text{O}_3$ for spectrofluorimetric determination of iron.

Table S3. Student t-test for statistical evaluation of accuracy.

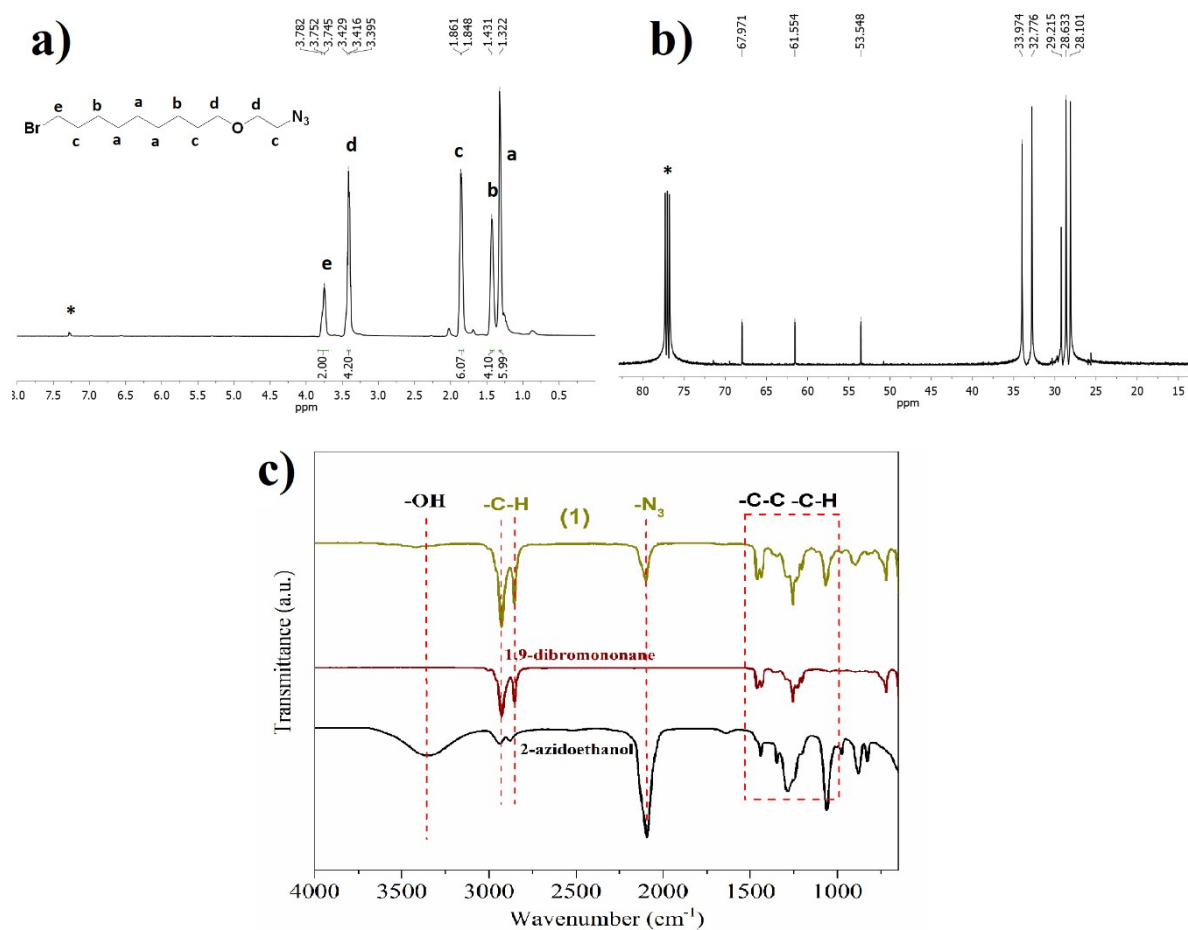


Figure S1: a) ^1H NMR, **b)** ^{13}C NMR and **c)** FTIR spectra of compound **1**. (NMR spectra were recorded in CDCl_3).

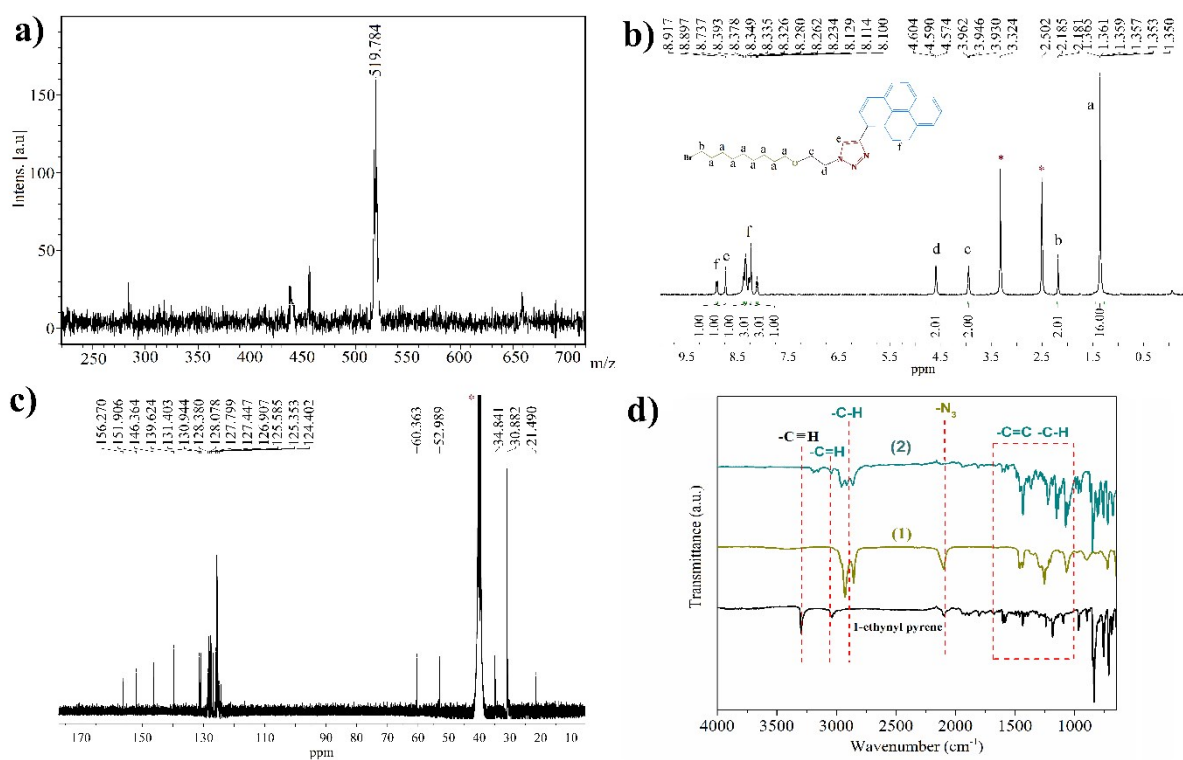


Figure S2: a) MALDI-TOF **b)** ^1H NMR, **c)** ^{13}C NMR and **d)** FTIR spectra of compound 2. (MALDI-MS spectrum was obtained with dithranol matrix and NMR spectra were recorded in DMSO-d_6).

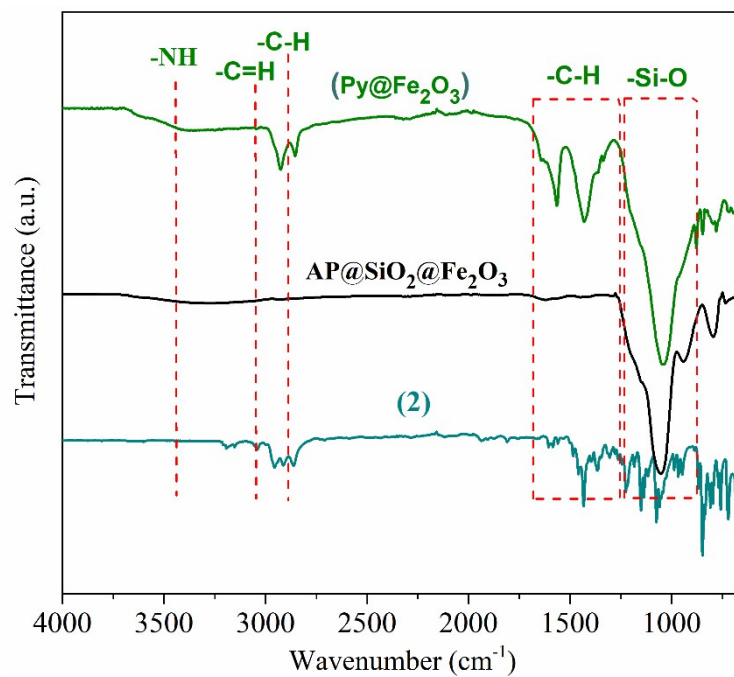


Figure S3: FTIR spectra of compound **2**, $\text{AP}@SiO_2@Fe_2O_3$, $\text{Py}@Fe_2O_3$ hybrid nanosensor.

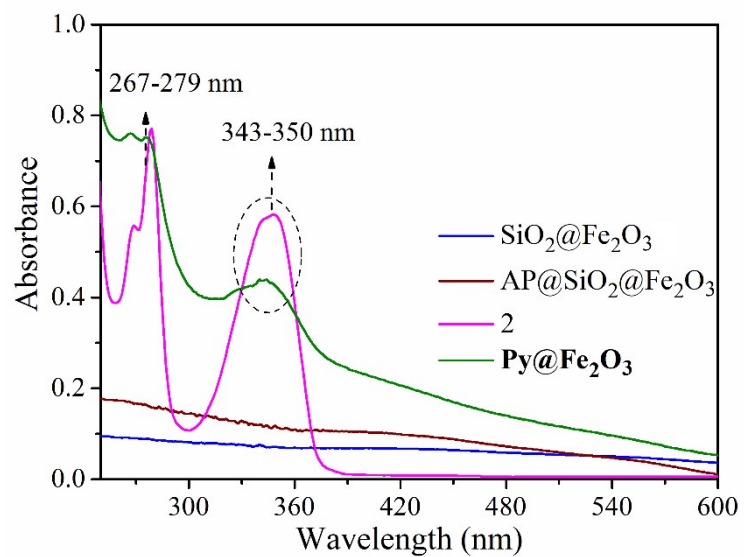


Figure S4: UV-Vis spectra of compound **2**, SiO₂@Fe₂O₃, AP@SiO₂@Fe₂O₃, **Py@Fe₂O₃** hybrid nanosensor.

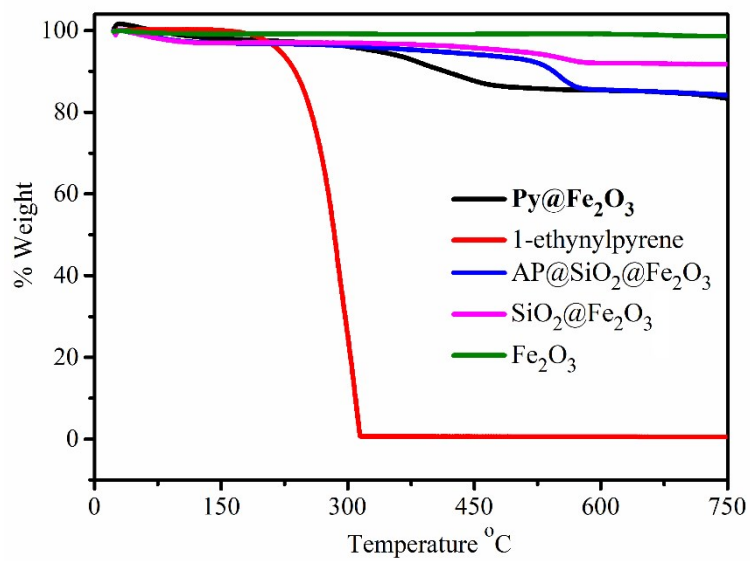


Figure S5: TGA thermograms of compound **2**, Fe₂O₃, SiO₂@Fe₂O₃, AP@SiO₂@Fe₂O₃, Py@Fe₂O₃ hybrid nanosensor.

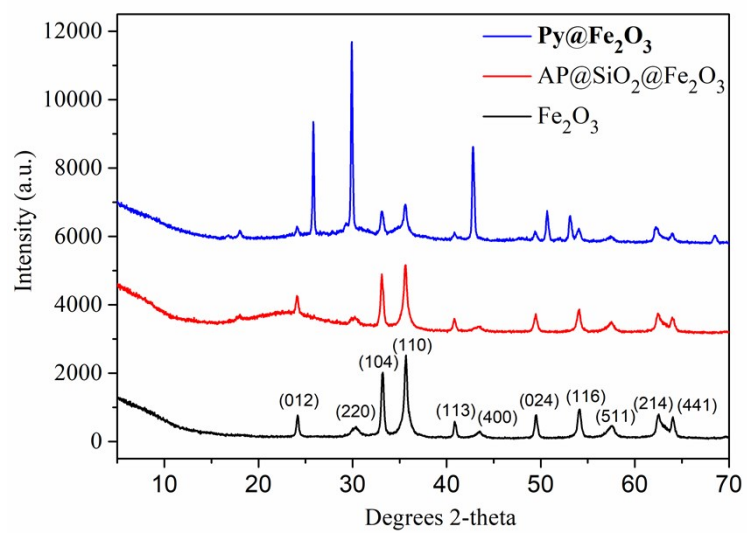


Figure S6. XRD patterns of Fe_2O_3 , $\text{AP@SiO}_2\text{@Fe}_2\text{O}_3$, $\text{Py@Fe}_2\text{O}_3$.

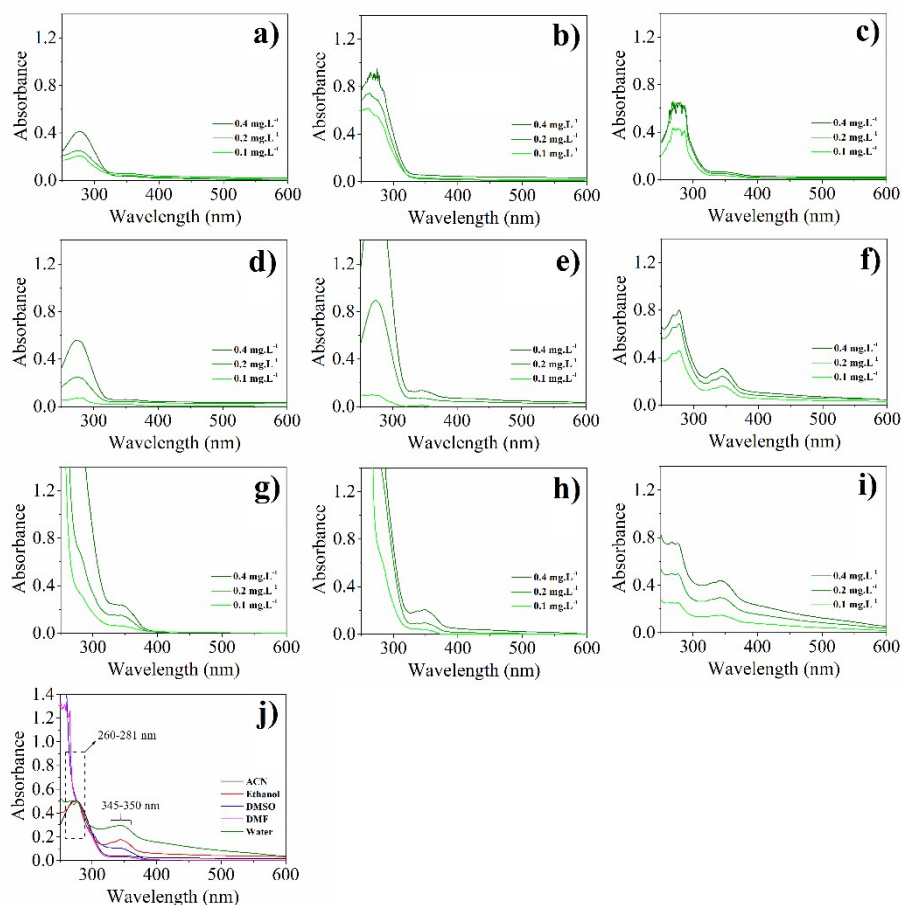


Figure S7. UV-Vis absorption of $\text{Py@Fe}_2\text{O}_3$ in **a)** hexane, **b)** 1,4-dioxane, **c)** THF, **d)** dichloromethane, **e)** ACN, **f)** ethanol, **g)** DMSO, **h)** DMF, **i)** water in different concentration and **j)** normalized absorption spectra of $\text{Py@Fe}_2\text{O}_3$ in different solvents.

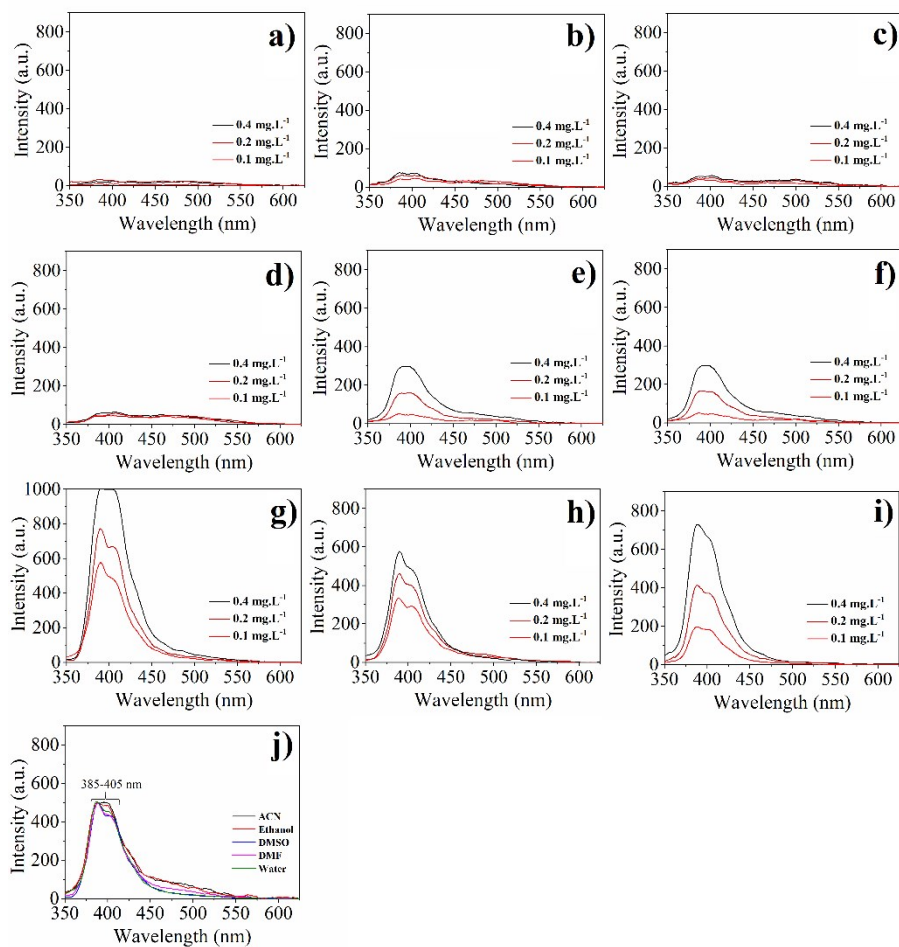


Figure S8. Fluorescence spectra of Py@Fe₂O₃ in **a)** hexane, **b)** 1,4-dioxane, **c)** THF, **d)** dichloromethane, **e)** ACN, **f)** ethanol, **g)** DMSO, **h)** DMF, **i)** water in different concentration and **j)** normalized fluorescence spectra of Py@Fe₂O₃ in different solvents.

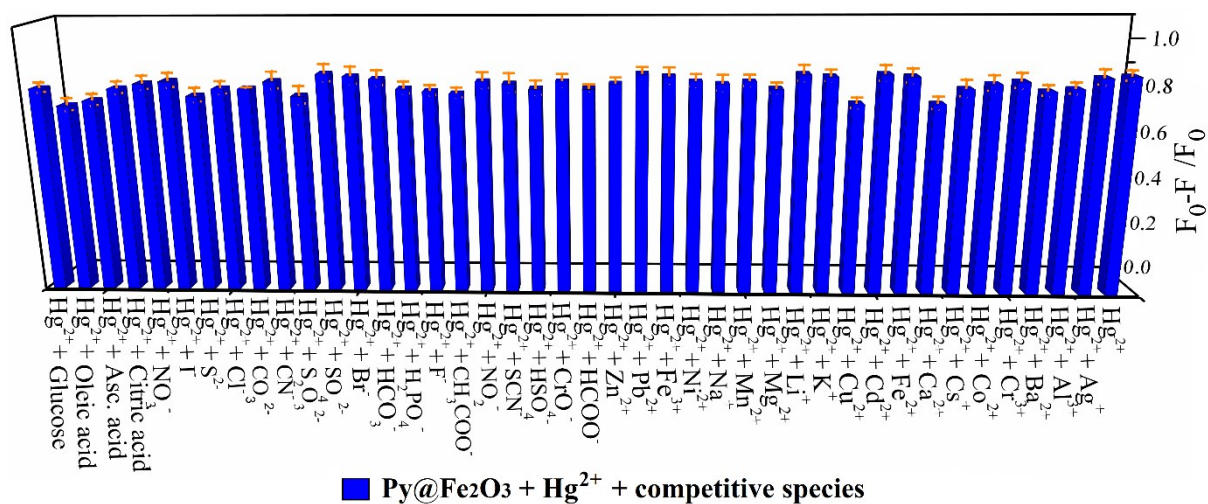


Figure S9. Interfering studies for 0.4 mg.mL⁻¹ Py@Fe₂O₃ in presence of 1.0 μmol.L⁻¹ Hg²⁺ after addition of 10 μmol.L⁻¹ various competitive species (pH of 8.0, λ_{ex}=325 nm, and slit width = 5 nm).

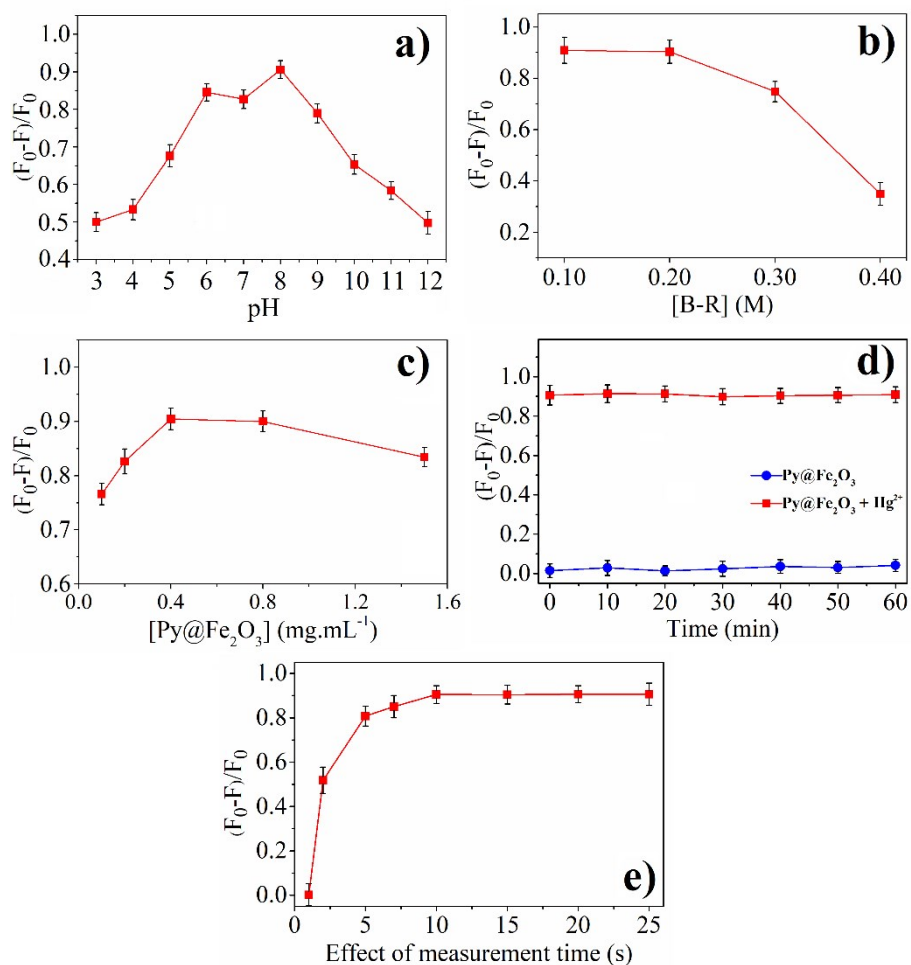


Figure S10. Effect of **a)** pH, **b)** buffer concentration, **c)** $\text{Py}@Fe_2O_3$ concentration, **d)** photostability and **e)** measurement time at pH of 8.0, $\lambda_{\text{ex}}=325$ nm, $0.4 \text{ mg}\cdot\text{mL}^{-1}$ of $\text{Py}@Fe_2O_3$ and $1.0 \mu\text{mol}\cdot\text{L}^{-1} Hg^{2+}$, and slit width = 5 nm).

Table S1: Photophysical parameters of **Py@Fe₂O₃**.

ϵ (mL.g ⁻¹ .cm ⁻¹) x10 ³									λ_{abs}	λ_{ems}	τ_0 (ns)	Φ_F
*Water	DMF	DMSO	DCM	EtOH	ACN	THF	Dxn	Hxn	(nm)	(nm)		
1.465	0.465	0.745	0.206	1.205	0.345	0.250	0.119	0.288	272	388	0.343±0.08	0.230
									345			

*Hxn, n-hexane; Dxn, 1,4-dioxane; THF, tetrahydrofuran; DCM, dichloromethane; ACN, acetonitrile; EtOH, ethanol; DMSO; dimethyl sulfoxide, DMF; dimethylformamide.

Table S2. Optimum conditions of **Py@Fe₂O₃** for spectrofluorimetric determination of iron.

Parameter	Value
Exc. (nm)	325
Ems. (nm)	388
LOD (nmol.L ⁻¹)	3.650
LOQ (nmol.L ⁻¹)	10.960
Linear range (μmol.L ⁻¹)	0.010-1.000
pH	8.0
Sensor concentration (mg.mL ⁻¹)	0.4
Final volume (mL)	5
Working media	water
Interaction time (second)	10
R ²	0.9976
RSD%	3.52

Table S3. Student t-test for statistical evaluation of accuracy.

Hg²⁺	s	X_R	\bar{X}	$t_{\text{exp.}} = \frac{ X_R - \bar{X} }{s/\sqrt{N}}$	t_{ref.}	Results
River water	2.59	1.819	2.006	0.13	4.3	0.13<4.3 (acceptable)
Mineral water	2.33	1.581	1.504	0.06	4.3	0.06<4.3 (acceptable)
Wastewater	2.08	12.280	12.030	0.21	4.3	0.21<4.3 (acceptable)